2970 *Chem. Mater.* **2010,** *22,* 2970–2977
DOI:10.1021/cm1003752

CHEMISTRY OF MATERIALS
Article

Fluorescence Spectroscopy Studies of Silica Film Polarity Gradients Prepared by Infusion-Withdrawal Dip-Coating

Fangmao Ye,[†] Chenchen Cui,[†] Alec Kirkeminde,[†] Dong Dong,[‡] Maryanne M. Collinson,*[,‡] and Daniel A. Higgins*[,†]

[†]*Department of Chemistry, Kansas State University, Manhattan, Kansas 66506, and* [‡]*Department of Chemistry, Virginia Commonwealth University, Richmond, Virginia 23284*

Received February 5, 2010

The preparation of sol−gel-derived silica films incorporating macroscopic polarity gradients is reported for the first time. Such materials are likely to find broad applications in chemical separations, combinatorial catalysis, and biological sensing. Polarity gradients were prepared by an "infusion-withdrawal dip-coating" procedure that produces a sol of time-varying composition. Tetramethoxysilane (TMOS) and methyltrimethoxysilane (MTMOS) were employed as the precursor silanes. Gradient deposition was accomplished by first suspending a substrate in a TMOS-derived sol. Synchronized syringe pumps were then used to slowly infuse a MTMOS sol into the deposition reservoir while the mixed sol was simultaneously withdrawn at a higher rate. The difference in infusion and withdrawal rates caused the sol to slowly recede down the substrate surface, mimicking a dip-coating process. Film polarity was characterized by doping the films with Nile Red (NR), a fluorescent, polarity-sensitive probe. NR fluorescence spectra acquired as a function of position along the films provide strong evidence for the presence of macroscopic, unidirectional polarity gradients in these materials. As expected, more polar environments are found at the top of each film and less polar environments at the bottom. Water contact angle data provide supporting evidence, consistent with the presence of a polarity gradient.

Introduction

The preparation of films and surfaces incorporating physical and chemical (i.e., compositional) gradients is a topic of contemporary scientific interest.[1−10] "Functionally graded" materials,[7] incorporating gradients in polarity, porosity, ionic site density, thickness, molecular weight, etc.,[1,6,8−10] have potential applications as stationary phases for chemical separations,[2] as materials for combinatorial catalysis,[11] and as absorbent/adsorbent layers for use in chemical or biological sensors.[12] Related surface gradients have been used to regulate adhesion of cells,[3,13,14] direct the growth of neurons,[3] and even drive the transport of liquids.[15]

A wide variety of approaches have been used to prepare gradient materials.[4,5] Representative examples include solution[16] and gas phase[17] surface modification of organic polymers; deposition of polymers from prepolymer solutions;[18,19] solution and vapor phase diffusion and surface modification using alkanethiols[12,13] and organosilanes;[15,20] and deposition of polymers[10,21] and manipulation of surface reactive species[1,9] by electrochemical means. Of the range of possible approaches, some of the simplest and most common involve dip-coating.[4] Additional examples and further discussion of alternative methods and materials can be found in recent reviews on soft matter gradients.[4,5] The methods described in these reviews constitute an extensive toolbox for the spatial and temporal control of materials properties. However, the continued exploration and implementation

*Corresponding author. E-mail: mmcollinson@vcu.edu (M.M.C.); higgins@ksu.edu (D.A.H.).

(1) Balss, K. M.; Coleman, B. D.; Lansford, C. H.; Haasch, R. T.; Bohn, P. W. *J. Phys. Chem. B* **2001**, *105*, 8970–8978.
(2) Cabrera, C. R.; Finlayson, B.; Yager, P. *Anal. Chem.* **2000**, *73*, 658–666.
(3) Dertinger, S. K. W.; Jiang, X.; Li, Z.; Murthy, V. N.; Whitesides, G. M. *Proc. Natl. Acad. Sci. U.S.A.* **2002**, *99*, 12542–12547.
(4) Genzer, J.; Bhat, R. R. *Langmuir* **2008**, *24*, 2294–2317.
(5) Morgenthaler, S.; Zink, C.; Spencer, N. D. *Soft Matter* **2008**, *4*, 419–434.
(6) May, E. L.; Hillier, A. C. *Anal. Chem.* **2005**, *77*, 6487–6493.
(7) Neubrand, A. *J. Appl. Electrochem.* **1998**, *28*, 1179–1188.
(8) Plummer, S. T.; Bohn, P. W. *Langmuir* **2002**, *18*, 4142–4149.
(9) Terrill, R. H.; Balss, K. M.; Zhang, Y.; Bohn, P. W. *J. Am. Chem. Soc.* **2000**, *122*, 988–989.
(10) Wang, X.; Haasch, R. T.; Bohn, P. W. *Langmuir* **2005**, *21*, 8452–8459.
(11) Senkan, S. *Angew. Chem., Int. Ed.* **2001**, *40*, 312–329.
(12) Liedberg, B.; Tengvall, P. *Langmuir* **1995**, *11*, 3821–3827.
(13) Mougin, K.; Ham, A. S.; Lawrence, M. B.; Fernandez, E. J.; Hillier, A. C. *Langmuir* **2005**, *21*, 4809–4812.
(14) Wang, Q.; Jakubowski, J. A.; Sweedler, J. V.; Bohn, P. W. *Anal. Chem.* **2004**, *76*, 1–8.
(15) Chaudhury, M. K.; Whitesides, G. M. *Science* **1992**, *256*, 1539–1541.
(16) Ueda-Yukoshi, T.; Matsuda, T. *Langmuir* **1995**, *11*, 4135–4140.
(17) Wijesundara, M. B. J.; Fuoco, E.; Hanley, L. *Langmuir* **2001**, *17*, 5721–5726.
(18) Xu, C.; Wu, T.; Mei, Y.; Drain, C. M.; Batteas, J. D.; Beers, K. L. *Langmuir* **2005**, *21*, 11136–11140.
(19) Tomlinson, M. R.; Efimenko, K.; Genzer, J. *Macromolecules* **2006**, *39*, 9049–9056.
(20) Elwing, H.; Welin, S.; Askendal, A.; Nilsson, U.; Lundstrom, I. *J. Colloid Interface Sci.* **1987**, *119*, 203–210.
(21) Wang, X.; Bohn, P. W. *J. Am. Chem. Soc.* **2004**, *126*, 6825–6832.

Published on Web 04/14/2010

of alternative materials chemistries in the preparation of gradients is also required if the true potential of these methods is to be fully realized. As eloquently stated by Wang, Haasch, and Bohn "... the utility of anisotropic in-plane gradient surfaces scales directly with the range of chemical and physical properties that can be accessed and manipulated ..."[10]

The sol−gel process[22−24] represents an important and convenient route to the preparation of a virtually unlimited range of materials having a wide range of physicochemical properties. Although simple silica materials can be prepared via the acid-catalyzed hydrolysis and condensation of tetramethoxysilane (TMOS),[22−24] more complex organic−inorganic hybrid materials can be prepared using mixed sols containing one or more organoalkoxysilanes (R'-Si(OR)$_3$, where R and R′ represent organic groups).[25−27] In this work, we show for the first time how temporal control over the sol composition can be utilized to prepare thin silica films with functionally graded properties. The range of gradients that can be prepared by this approach is virtually unlimited due to the enormous selection of commercially available organoalkoxysilanes. Importantly, materials composition and properties can be altered by simply changing the precursors employed. In spite of its potential utility, the sol−gel process has seldom been employed in the preparation of gradient materials[28] and much remains to be learned about the range of materials and properties that can be accessed.

In this paper, an "infusion-withdrawal dip-coating" process is employed for the preparation of silica films incorporating macroscopic polarity gradients. Glass and silicon substrates were coated with sols of time-varying composition produced by slowly mixing TMOS- and MTMOS-based sols together. The time-varying sol composition led to a steady decrease in film polarity along the substrate surface. The gradients thus prepared were characterized by fluorescence spectroscopy, using Nile Red (NR). NR was selected because its fluorescence emission is highly sensitive to materials polarity[29,30] and because it has been used previously for characterization of sol−gel-derived materials in both ensemble[31] and single molecule[32,33] spectroscopic studies. Water contact angle measurements[15,16,34,35] were used to obtain supporting evidence for gradient formation. The fluorescence spectra obtained from NR-doped films exhibited a monotonic, position-dependent blue shift from the top of the film to the bottom, indicative of a decrease in film polarity from top to bottom. Similarly, water contact angle measurements showed a monotonic increase in the contact angle from top to bottom.

Experimental Section

Sample Preparation. Glass coverslips (Fisher Premium) and silicon wafers (Silicon Inc.) were both employed as substrates. Prior to use, all substrates were cleaned in fresh Piranha solution (***Caution***: *Piranha solutions are extremely dangerous and react violently with organic materials*); they were subsequently cleaned a second time in an air plasma. This two-step process ensured rigorous removal of all organic contaminants.

Adhesion of the precursor alkoxysilanes during gradient deposition was improved by first coating the substrates with a silica sublayer. Tetramethoxysilane (99%, TMOS, Fisher) sols were prepared for this purpose in a 1:11.5:5.1:0.006 (TMOS:H_2O:Ethanol:HCl(0.1 M)) mole ratio and were allowed to age for 1 day prior to use. The clean substrates were subsequently spin-coated with these sols and dried in a desiccator for 1 day. The resulting coatings were uniform and had thicknesses of ∼180 nm, as determined by both profilometry and ellipsometry.

Production of silica film polarity gradients employed a time-varying mixture of two different sols. The first was a TMOS sol prepared in a 1:80:5.3:0.095 (TMOS:Ethanol:H_2O:NH_4OH(1 M)) mole ratio and subsequently aged for 6 h. The second was any of several different sols prepared using methyltrimethoxysilane (97%, MTMOS, Fisher). Typically, sols were prepared using different volumes of ethanol and constant water concentration. These sols were prepared in 1:10:4:0.072, 1:20:8:0.072, and 1:40:13:0.072 (MTMOS:Ethanol:H_2O:NH_4OH(1 M)) mole ratios and were aged for 6 h. The sol aging time was selected after experimentation with sols aged for both shorter and longer times. Shorter aging times yielded thinner films, whereas longer times yielded films of increased thickness and roughness. It was concluded that 6 h aging yielded the most acceptable films (i.e., of reasonable thickness and relatively small roughness). All sols are designated throughout this manuscript by their silane to ethanol mole ratios, i.e., as 1:10, 1:20, and 1:40 MTMOS sols.

Gradient films were deposited on the sublayer-coated substrates in a custom built glass reservoir designed to simultaneously minimize sol volume, decrease sol evaporation and allow for stirring of the sol mixture. A diagram of the apparatus and a photograph of the reservoir are shown in Figure 1. The glass reservoir includes a rectangular upper region having dimensions of 3.5 cm × 0.5 cm × 3.0 cm ($L \times W \times H$) that was designed to admit one-inch-wide substrates. The lower portion of the reservoir was comprised of a small cylindrical vial (D = 1 cm, H = 1 cm). Two small glass tubes were installed at fixed locations inside the reservoir for infusion and withdrawal of the sols. All depositions were performed with the reservoir mounted atop a pneumatic vibration isolation table, with the reservoir housed in a closed Plexiglas box maintained at ∼50% relative humidity and ∼20 °C.

(22) Brinker, C. J.; Scherer, G. W. *Sol−Gel Science: The Physics and Chemistry of Sol−Gel Processing*; Academic Press: Boston, 1990.
(23) Avnir, D. *Acc. Chem. Res.* **1995**, *28*, 328–334.
(24) Collinson, M. M. In *Chalcogenide Glasses and Sol−Gel Materials*; Nalwa, H. S., Ed.; Academic Press: New York, 2001; Vol. *5*, pp 163−194.
(25) Schmidt, H. *J. Sol−Gel Sci. Technol.* **1994**, *1*, 217–231.
(26) Wen, J.; Wilkes, G. L. *Chem. Mater.* **1996**, *8*, 1667–1681.
(27) Collinson, M. M. *Trends Anal. Chem.* **2002**, *21*, 30–38.
(28) Thierry, T.; Bruno, B.; Christian, F. *J. Appl. Polym. Sci.* **2007**, *104*, 1504–1516.
(29) Deye, J. F.; Berger, T. A.; Anderson, A. G. *Anal. Chem.* **1990**, *62*, 615–622.
(30) Hou, Y.; Bardo, A. M.; Martinez, C.; Higgins, D. A. *J. Phys. Chem. B* **2000**, *104*, 212–219.
(31) Lobnik, A.; Wolfbeis, O. S. *J. Sol−Gel Sci. Technol.* **2001**, *20*, 303–311.
(32) Bardo, A. M.; Collinson, M. M.; Higgins, D. A. *Chem. Mater.* **2001**, *13*, 2713–2721.
(33) Higgins, D. A.; Collinson, M. M.; Saroja, G.; Bardo, A. M. *Chem. Mater.* **2002**, *14*, 3734–3744.
(34) Morgenthaler, S.; Lee, S.; Zurcher, S.; Spencer, N. D. *Langmuir* **2003**, *19*, 10459–10462.
(35) Yu, X.; Wang, Z.; Jiang, Y.; Zhang, X. *Langmuir* **2006**, *22*, 4483–4486.

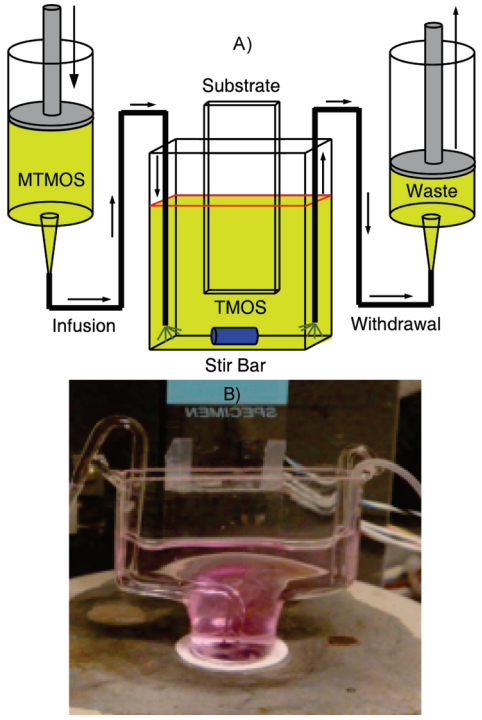

Figure 1. (A) Diagram of "infusion-withdrawal dip-coating" apparatus used to prepare silica film gradients and (B) photograph of the deposition reservoir. Synchronized syringe pumps are used to (1) infuse an MTMOS sol into the (initially) TMOS-filled reservoir and (2) withdraw the resulting mixed sol from the reservoir. The withdrawal rate is set faster than infusion so that the sol slowly recedes down the face of the substrate.

Deposition of silica film polarity gradients was accomplished as follows. A sublayer-coated substrate was first suspended in the middle of the reservoir. The initial TMOS sol was then transferred into the reservoir, submersing all but the top 2−3 mm of the substrate. The MTMOS sol selected for a given deposition was then loaded into a syringe, which was mounted in a syringe pump (NE-1000, New Era Pump Systems, Inc.). The syringe was attached to the reservoir via flexible plastic tubing. Gradient deposition proceeded by slowly infusing the MTMOS sol into the reservoir. The mixed sol contained in the reservoir was simultaneously withdrawn using a second, synchronized syringe pump also attached to the reservoir through flexible plastic tubing. The infusion pump was set to deliver MTMOS sol at a rate of 10.0 mL/h, while the other was set to withdraw 14.2 mL/h of mixed sol. The sol within the reservoir was carefully stirred at a constant rate, using a magnetic stir bar throughout this process. Prior to the start of deposition, it was verified that sol stirring produced no detectable movement of the sol surface. The difference in infusion and withdrawal rates led to a steady decrease in the height ($\sim$ 0.3 mm/min) of the sol in the reservoir. The entire "infusion-withdrawal dip-coating" process lasted for $\sim$1 h, producing an overall change of $\sim$1.2 − 1.5 cm in sol height. After deposition, residual sol clinging to the bottom of the substrate was gently removed using a Kimwipe. The final gradient films were dried in a desiccator for 1−2 days.

Preparation of dye-doped silica gradients was performed on sublayer-coated glass coverslips and proceeded exactly as described above, except that both sols incorporated Nile Red (NR) at $\sim$1 μM concentration. In some cases, gradients were simultaneously prepared on two coverslips, using the same sol mixture. In this case, the two substrates were assembled back-to-back with a thin film of glycerin between them. The thin layer of glycerin prevented silica deposition on the backside of the substrates. Without the glycerin layer, inadvertent coating of the substrate backside was found to interfere with the determination of polarity properties from the NR emission.

Nongradient silica films having uniform composition and polarity properties were prepared to aid in interpretation of data obtained from the gradients. For this purpose, TMOS (TMOS:H_2O:ethanol:NH_4OH = 1:80:5.3:0.095) and MTMOS (MTMOS:ethanol:H_2O:NH_4OH = 1:10:4:0.072) sols were prepared as described above and aged for 6 h. One- and two-component sols containing different mole fractions of TMOS and MTMOS were then obtained by mixing appropriate amounts of each of these sols. Sols containing 0, 20, 40, 60, 80, and 100% MTMOS (relative to total silica content) were prepared and vigorously mixed for 20 min. These sol mixtures were then either spin-coated (100 μL, 5000 rpm, 30 s) or dip-coated onto both clean and sublayer-coated substrates. Dip-coating of these sols employed the same apparatus and similar methods employed to prepare gradient films. In this case, a single syringe pump was used to slowly withdraw sol from the deposition reservoir. All such films were dried in a desiccator at room temperature for 1−2 days prior to use.

Characterization. The thickness of each sample was characterized on a macroscopic scale by spectroscopic ellipsometry (α-SE, J.A. Woollam), whereas thickness and roughness on a microscopic scale were characterized by surface profilometry (XP-2, Ambios Technology; Santa Cruz, CA). All ellipsometric measurements were performed on samples cast on silicon substrates, whereas profilometry data were acquired from films cast on both glass and silicon substrates.

Spectroscopic ellipsometry has been employed previously for characterization of film thickness and optical constants in multilayer[36] and nonuniform gradient[37] films. To determine film thickness as a function of position, ellipsometric data were acquired at 1($\pm$0.2) mm intervals along the films. Data were acquired from approximately the same locations (i.e., within $\pm$0.2 mm) both before (TMOS sublayer alone) and after gradient deposition. The films were modeled as transparent layers on silicon, with dispersion in the films described by the Cauchy relationship.[36] Data obtained from TMOS sublayers alone could all be modeled with similar parameters (e.g., Cauchy A parameter = 1.426, B = 0.00698, and C = −0.00049). The gradient overlayers were modeled as a second layer atop the TMOS sublayer (Cauchy A parameter = 1.25, with B, C, and gradient thickness adjusted to fit the data). In all cases, the film thickness values determined by ellipsometry were consistent with those obtained from profilometry measurements.

Static sessile-drop water contact angle measurements were performed on a home-built apparatus run by software written in-house. A Navitar camera was used to record droplet images. In these experiments, 2.5 μL drops of deionized water were deposited at regular intervals on the samples. Images were acquired 3 s after addition of each drop to the sample surface, allowing for stabilization of the contact angle. Automated routines incorporated into the instrument software were used to determine contact angles.

Fluorescence spectra were obtained from NR-doped gradient and nongradient films using a home-built fluorescence microscope. Light ($\sim$1 μW) from a green HeNe laser (543.5 nm) was used to excite fluorescence in the samples. This light was focused

(36) Langereis, E.; Heil, S. B. S.; Knoops, H. C. M.; Keuning, W.; van de Sanden, M. C. M.; Kessels, W. M. M. *J. Phys. D: Appl. Phys.* **2009**, *42*, 073001.
(37) Aulika, I.; Dejneka, A.; Zauls, V.; Kundzins, K. *J. Electrochem. Soc.* **2008**, *155*, G209–G213.

into the back aperture of a 50× (0.55 numerical aperture) air objective, producing a 20 μm diameter spot in the sample. The same objective was used to collect the sample fluorescence and direct it through a holographic notch filter (Kaiser Optical) and into a 0.15 m spectrograph (Acton Research). A liquid-N_2-cooled CCD (Princeton Instruments) was used to record the spectra. Spectra were taken every 1(±0.2) mm along gradient samples, using a 30 s integration time.

Results and Discussion

Model for Sol Composition. The "infusion-withdrawal dip-coating" procedure employed in gradient preparation produces a sol of time-varying composition. Predictions of the sol composition at each instant in time can be readily obtained from a simple mathematical model of the process. The rates of change for the TMOS and MTMOS concentrations in the deposition reservoir are defined by the following two differential equations:

$$\frac{dC_{TMOS}(t)}{dt} = -\frac{C_{TMOS}(t)F_{out}}{V_{sol}(t=0)-(F_{out}-F_{in})t} \quad (1)$$

$$\frac{dC_{MTMOS}(t)}{dt} = \frac{C_{MTMOS,b}F_{in}-C_{MTMOS}(t)F_{out}}{V_{sol}(t=0)-(F_{out}-F_{in})t} \quad (2)$$

Here, $V_{sol}(t = 0)$ is the initial sol volume (10 mL) in the deposition reservoir. $C_{TMOS}(t)$ and $C_{MTMOS}(t)$ represent the time-dependent concentrations of TMOS and MTMOS in the reservoir, whereas $C_{MTMOS,b}$ represents the time invariant concentration of MTMOS in the infusion sol. Finally, F_{in} and F_{out} are the volume flow rates for the infusion and withdrawal processes. Solution of the above two equations yields the following expressions describing $C_{TMOS}(t)$ and $C_{MTMOS}(t)$

$$C_{TMOS}(t) = C_{TMOS}(t=0)\left(\frac{V_{sol}(t)}{V_{sol}(t=0)}\right)^{F_{out}/(F_{out}-F_{in})} \quad (3)$$

$$C_{MTMOS}(t) = C_{MTMOS,b}\frac{F_{in}}{F_{out}}\left(1-\left(\frac{V_{sol}(t)}{V_{sol}(t=0)}\right)^{F_{out}/(F_{out}-F_{in})}\right) \quad (4)$$

where, $V_{sol}(t)$ is the instantaneous sol volume in the reservoir (i.e., $V_{sol}(t = 0) - (F_{out} - F_{in})t$). The results of these calculations were subsequently used to determine the time-dependent mole fraction, $R_{MTMOS}(t) = C_{MTMOS}(t)/(C_{MTMOS}(t) + C_{TMOS}(t))$, of MTMOS in the sol. Figure 2 plots these results for different MTMOS sol concentrations (i.e., for 1:10, 1:20, and 1:40 MTMOS sols). As shown in the figure, different recipes are expected to yield sols of slightly different compositions, suggesting that gradients having different compositional properties can be prepared.

Optical Inspection of Films. Optical inspection was employed to judge the overall quality of the gradient films obtained. Figure 3A shows a representative photograph of a gradient on a sublayer-coated silicon substrate. This particular film was derived from a 1:10 MTMOS sol. It is 1.3 cm wide and the gradient is 1.8 cm in length. It is most noteworthy that a general trend from dark to light is observed from top to bottom along the gradient film. Colorful interference lines are also observed. These run across the film (i.e., perpendicular to the gradient dimension) and appear at "random" locations along the gradient. Observation of the sol during dip-coating indicated that the sol surface was free from any vibrations that might cause such lines. Furthermore, films deposited without stirring also exhibited interference lines. Because gradient deposition was performed on a pneumatic vibration isolation table and in a closed Plexiglas chamber, it is unlikely that mechanical vibrations and air currents caused these lines. Extensive additional studies performed with a conventional dip-coater suggest their appearance is directly related to the sol deposition mechanism and therefore cannot be easily eliminated. The appearance of the interference lines will be discussed further, below. Here, it is sufficient to note that film thickness variations as small as a few tens of nanometers[38] can result in color changes similar to those observed.

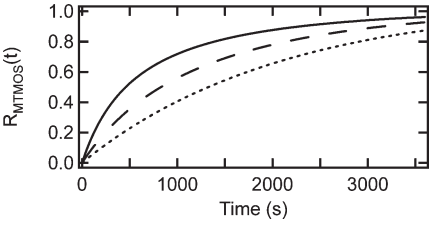

Figure 2. Plots of time-dependent $R_{MTMOS}(t)$ for 1:10 (solid line), 1:20 (dashed line), and 1:40 (dotted line) MTMOS sols.

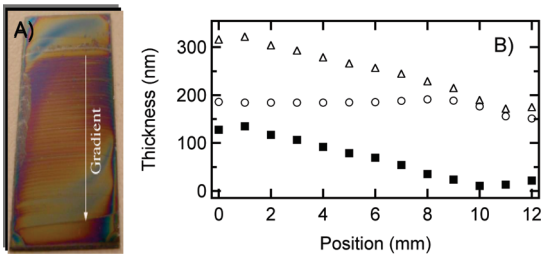

Figure 3. (A) Photograph of a silica film gradient on a silicon wafer (with TMOS sublayer). (B) Position-dependent thickness determined by ellipsometry for a gradient prepared by "infusion-withdrawal dip-coating" using a 1:10 MTMOS sol. Overall film thickness (open triangles), thickness of TMOS-coated substrate (open circles), and gradient thickness (solid squares) are shown.

Film Thickness and Surface Roughness. The thicknesses of the TMOS sublayers and gradient films cast on silicon substrates were determined using spectroscopic ellipsometry. Film thickness was measured at 1 mm intervals both before and after gradient deposition in approximately the same locations (i.e., within ±0.2 mm) in each case. Figure 3B shows representative position-dependent thickness data acquired from a 1:10 MTMOS gradient. Shown are thickness values for the overall film, the

(38) Hecht, E. *Optics*; Addison-Wesley: Reading, MA, 1987.

TMOS sublayer, and the gradient itself. Surface profilometry measurements performed on similarly prepared films yielded thickness values consistent with all ellipsometry data. These data show that the TMOS sublayer is relatively uniform across the substrate and ~180 nm thick. The gradient film, however, shows a clear decrease in average thickness along the gradient dimension. In this sample, the gradient film thickness is greatest at the top, yielding a value of ~130 nm, and gradually decreases to ~10 nm thick at the bottom. Gradients prepared from 1:20 and 1:40 MTMOS sols showed the same film thinning trends but no clear dependence in thickness on MTMOS sol concentration (data not shown). Film thinning is partly a result of variations in the influence of stirring (as the deposition region gradually approaches the stir bar) but could also include contributions from differences in the wetting of the sublayer by the time-varying mixed sol, differences in the degrees of hydrolysis and condensation of TMOS and MTMOS, differences in the rates at which these two precursors attach to the sublayer, or differences in the sol viscosities.[39,40] Future investigations will seek to better understand this phenomenon.

Surface roughness was determined by profilometry. Representative roughness data for a gradient prepared from a 1:10 MTMOS sol are shown in the Supporting Information (Figure S1). These data, taken together with other profiles acquired in several regions on a number of other films, depict a mean surface roughness of 12 ± 4 nm (root-mean-square, rms), as measured over 400 μm distances (20 measurements, 5 different samples). Surface roughness on this scale is dominated by features separated by ~50 μm (on average) and running across the film. On a larger scale, the roughness is dominated by features (not shown) of millimeter spacing, also running across the film. These features correspond well with the lines observed in the optical images (see Figure 3), indicating that the height (i.e., film thickness) variations observed are the cause of the colorful interference lines. Importantly, as shown in Figure S1 in the Supporting Information, the roughness does not vary dramatically across the gradient. Analysis of data from several samples indicates the roughness at the top of the gradient is, on average, ~ 50% greater than at the bottom.

The exact origins of the randomly positioned film thickness variations and interference lines are unknown at present. However, after extensive experimentation and consideration of published literature, it is very likely that they result from a combination of the sol deposition mechanism described by Brinker[39,40] and the pinning and release (i.e., stick−slip) of the sol contact line with the substrate surface.[41]

As described by Brinker and co-workers,[39,40] sol deposition during dip-coating occurs primarily in the upper regions of the meniscus formed at the sol−substrate−air interface. In this region, evaporation of solvent (primarily ethanol)[39] and capillary flow[42] leads to concentration of the silica precursors and water at the top of the meniscus.[40] As a result of the high silica and water concentrations, hydrolysis and condensation, and hence silica deposition, occur most rapidly in this region. Relatively little silica deposits on the substrate from the bulk of the sol.

It is commonly expected that the meniscus recedes down the substrate at a uniform rate. However, the contact line between the sol and substrate may become briefly pinned at a fixed location, later releasing and rapidly dropping to a new location where it is again pinned. Such a "stick−slip" process provides a mechanism for delivery of variable quantities of silica precursor to the substrate surface during "infusion-withdrawal dip-coating." "Stick−slip" processes of this type have recently been used in contact-line printing experiments for controlled placement and organization of nanomaterials.[41] It is likely this same process leads to the small variations in film thickness (i.e., the interference lines) observed in the present silica film gradients. On the basis of this model, and after extensive experimentation, we have concluded that the ~12 nm rms roughness observed on 400 μm length scales is the best that can be achieved using the present methods.

Fluorescence Measurements of Film Polarity. The primary objective of the present work is to produce silica films incorporating polarity gradients. Polarity along the gradient direction in films prepared as described above was probed by entrapping the solvent-sensitive dye NR in the film. NR has been used in the past to probe the polarity properties of a wide range of liquid and solid environments.[29−33] It is one of the most solvent sensitive fluorescent probes, exhibiting a dramatic bathochromic shift (of ~100 nm) in its emission spectrum between nonpolar (i.e., hexane) and polar (i.e., water) solvents.[29] In the present experiments, NR was doped into both gradient and nongradient silica films at ~1 μM concentrations.

NR Emission from Nongradient Films. NR emission spectra were initially recorded for a series of nongradient TMOS and MTMOS films. These experiments provided valuable information on the NR emission characteristics for films of different polarities. Emission spectra were first acquired from single-component, nongradient films that had been prepared on TMOS sublayer-coated coverslips using dip-coating methods similar to those used in gradient preparation (see Experimental Section). The fluorescence emission maxima for TMOS and MTMOS derived films appeared at ~640 and ~618 nm, respectively, reflecting the significant polarity differences of these films. These emission maxima were found to be similar to those obtained from spin-coated TMOS and MTMOS films prepared both without and with TMOS

(39) Brinker, C. J.; Frye, G. C.; Hurd, A. J.; Ashley, C. S. *Thin Solid Films* **1991**, *201*, 97–108.
(40) Nishida, F.; McKiernan, J. M.; Dunn, B.; Zink, J. I.; Brinker, C. J.; Hurd, A. J. *J. Am. Ceram. Soc.* **1995**, *78*, 1640–1648.
(41) Huang, J.; Fan, R.; Connor, S.; Yang, P. *Angew. Chem., Int. Ed* **2007**, *46*, 2414–2417.
(42) Deegan, R. D.; Bakajin, O.; Dupont, T. F.; Huber, G.; Nagel, S. R.; Witten, T. A. *Nature* **1997**, *389*, 827–829.

sublayers (~ 650 and ~605 nm, and ~643 and ~615 nm, respectively). The shift in NR emission between spin-coated MTMOS films prepared without sublayers and those obtained by dip-coating on TMOS sublayers show that penetration of NR into the sublayer has only a modest effect on the results.

A series of one- and two-component, nongradient silica films derived from 0, 20, 40, 60, 80, and 100% MTMOS sols (relative to total silane) were also investigated. Emission spectra obtained as a function of MTMOS mole fraction in the nongradient films provide a clear view of the hypsochromic shift exhibited by NR upon a change from TMOS-derived films to MTMOS-derived films. Figure S2 (see Supporting Information) shows NR fluorescence spectra obtained from several different films prepared using different mole fractions of MTMOS. In order to more quantitatively assess the polarity characteristics observed for films prepared using different TMOS and MTMOS mole fractions, a "polarity fraction" (PF) was defined. The PF was calculated directly from the NR emission spectra by measuring the average NR fluorescence in 10 nm wide bands centered at 605 nm (reflecting nonpolar environments) and 650 nm (polar environments) and determining the fraction of the total emission that occurred in the 605 nm band. The PF is expected to increase with increasing methyl content of the films. PF values of 0.25 and 0.60 were obtained for nongradient spin-coated TMOS and MTMOS films (without sublayers), respectively.

Figure 4A plots the PF values obtained as a function of MTMOS mole fraction in nongradient films dip-coated onto TMOS-sublayer-coated substrates. A monotonic and nominally linear increase from 0.30 to 0.58 is observed in the PF value as the mole fraction of MTMOS in the dipping sol increases from 0 to 80%. The similarities in the PF values obtained from spin-coated and dip-coated films in the absence and presence, respectively, of a TMOS sublayer provides supporting evidence that the polarity results are not dramatically altered by penetration of the dye into the TMOS sublayer.

NR Emission from Gradient Films. NR spectra recorded from the gradient films clearly demonstrate the presence of a polarity gradient. The PF values obtained as a function of position along each of three different gradients are plotted in Figure 4B. Representative NR fluorescence spectra are shown in Figure 4C. The PF data show a clear monotonic increase from the top (0 mm) of the film to the bottom. The PF values obtained from the gradients are somewhat smaller than those of the dip-coated nongradient films. For example, the 1:10:4 MTMOS gradient exhibits an initial PF of 0.24, while a nongradient 0% MTMOS (100% TMOS) film yields 0.30. At the other end of the same gradient, a PF of 0.42 is obtained, whereas a nongradient 80% MTMOS film yields 0.58. These results suggest the gradient films are slightly more polar than the nongradient films. These polarity differences likely result from differences in the deposition process in each case. The nongradient films are deposited from a static, homogeneous mixture of two

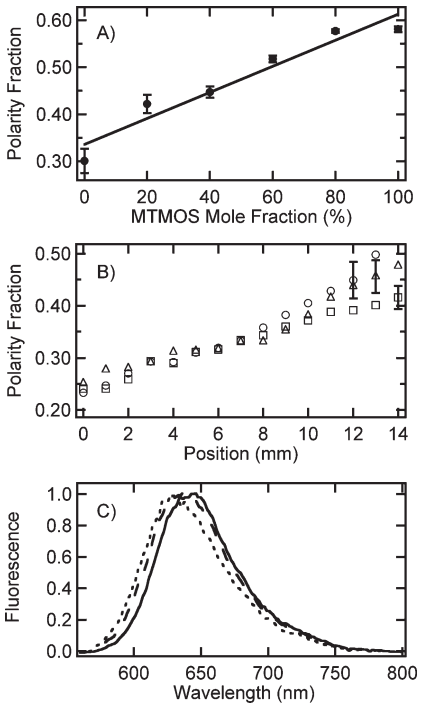

Figure 4. (A) Polarity fraction (PF) as a function of MTMOS mole fraction for one- and two-component nongradient (dip-coated) films. The solid line has been appended to better depict the trend in the data. (B) Polarity fraction as a function of position for gradient samples. The top of the gradient corresponds to 0 mm. Shown are data from 1:10 (open squares), 1:20 (open triangles) and 1:40 (open circles) MTMOS gradients. The error bars represent the average standard deviation obtained from measurements on at least three different samples in each case. (C) Representative NR fluorescence spectra (normalized) for a 1:10 MTMOS gradient taken from the top (solid line), middle (dashed line), and bottom (dotted line) of the gradient.

sols, whereas the gradients are deposited from a time-varying mixture, which never exactly duplicates the conditions under which the nongradient films were deposited. Nevertheless, all three gradients (see Figure 4B) show PF values that are similar to those of the nongradient films, suggesting similar variations in the methyl content of the gradients.

Interestingly, all three gradients show similar PF values (within experimental error) along their lengths, although the measured values become more variable toward the bottom of the gradients (see Figure 4B). As shown in Figure 2, the compositions of the sol mixtures from which the films were grown are expected to be distinctly different, with higher MTMOS concentrations leading to greater methyl content at intermediate times. Such differences in the sol composition would be expected to appear in the final films as well, with greater methyl content observed in intermediate gradient regions, when relatively high concentration MTMOS sols are employed. The apparent insensitivity of the gradients to MTMOS concentration is again attributable to the details of silica deposition. Differences in the MTMOS sols arise primarily from dilution with ethanol. Because ethanol evaporation occurs efficiently from the top of the meniscus,[39] the concentration of silica precursor in the deposition region is likely more similar than otherwise expected from the composition of the original sol. As a result, little

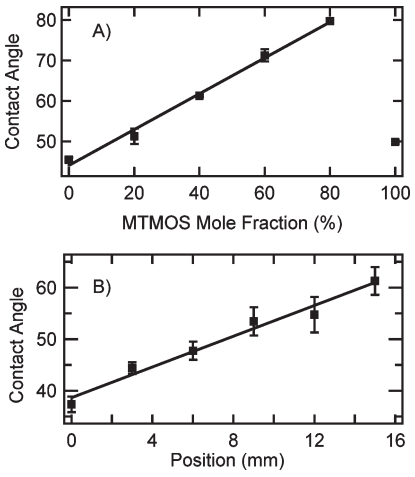

Figure 5. Contact angle in degrees for (A) one- and two-component nongradient (dip-coated) films and (B) a 1:40 MTMOS gradient, both on TMOS sublayer-coated substrates. The solid lines have been added to better depict trends in the data. The error bars show the standard deviations obtained from multiple measurements performed on each sample.

dependence of the final film properties (PF and thickness) on sol concentration is observed.

Water Contact Angle. Additional evidence for the formation of silica film gradients was obtained from sessile-drop water contact angle measurements.[15,16,34,35] The incorporation of methyl groups in sol−gel materials derived from MTMOS makes them more hydrophobic than those prepared from TMOS, leading to an expected increase in contact angle running down the gradient.

As in the fluorescence measurements described above, variations in the contact angle attributable to methyl modification were initially explored for one- and two-component nongradient films (dip-coated and spin-coated on TMOS-sublayer-coated substrates) prepared from sols of differing MTMOS and TMOS mole fractions. The results for dip-coated films are plotted in Figure 5A. A monotonic increase in water contact angle was observed for films derived from 0% to 80% MTMOS sols. For pure TMOS, the water contact angle was 45°, whereas for 80% MTMOS, it was 80°. A similar trend was observed for spin-coated nongradient films. These contact angle values are consistent with those reported previously for related "nonporous" sol−gel-derived silica films,[43−45] but are significantly smaller than those of porous MTMOS-derived superhydrophobic aerogels.[46,47] Deviation from the observed trend at 100% MTMOS is attributed to the formation of nonuniform/discontinuous films in this case. Film nonuniformity is evidenced by increased film roughness that is observable by eye.

Water contact angles were also measured as a function of position along each of the silica film gradients. Figure 5B plots representative contact angle results for a 1:40 MTMOS gradient. The gradient film shows a monotonic trend similar to that obtained from the non-gradient films, exhibiting contact angles of 37° at the top of the gradient, and 61° at the bottom. Data obtained on 1:10 films were indistinguishable from those obtained from 1:40 films. These data are consistent with the presence of a methyl-modified silica gradient running from top to bottom. The differences in contact angles obtained from gradient and nongradient films are attributed to differences in the preparation methods (i.e., time-varying sol mixtures in the former, homogeneous mixtures in the latter) and differences in surface roughness. It is well-known that variations in surface roughness can cause variations in the contact angle,[48,49] making quantitative comparisons between data sets difficult. Surface roughness specifically leads to observed contact angles that are smaller and larger, respectively, than expected on hydrophilic and hydrophobic surfaces.[48,49] As noted above, profilometry data shows the roughness is ~50% greater at the top of the gradient than at the bottom, suggesting the contact angles at the top of the gradient may be depressed due to increased roughness. It is concluded that although roughness variations may enhance the trend in contact angle along the gradients, these data remain consistent with the presence of a polarity gradient.

Conclusions

Silica thin films incorporating polarity gradients have been prepared for the first time using an "infusion-withdrawal dip-coating" procedure. The gradient is formed by immersing a substrate into a sol whose composition is varied as a function of time in a controlled fashion. Silica films incorporating spatially varying properties are deposited as the sol is withdrawn down the substrate surface. Results from fluorescence spectroscopy and contact angle measurements provide evidence that the films obtained incorporate polarity gradients derived from increasing concentrations of methyl-modified silica. Although in this work sols of time varying TMOS and MTMOS content were used to form polarity gradients on glass slides and silicon wafers, it is anticipated that the infusion-withdrawal dip-coating procedure could be used with nearly any combination of organoalkoxysilanes to prepare gradients whose composition/functionality gradually changes across the film. Polarity gradients like those prepared herein have a variety of potential applications as stationary phases for chemical separations, as solid supports for combinatorial catalysis and as supports for biological sensors. The continued development of sol−gel methods for producing silica film gradients will provide new routes to unique thin film materials of spatially controlled chemical and physical properties.

(43) Park, H. Y.; Kang, D. P.; Na, M. K.; Lee, H. W.; Lee, H. H.; Shin, D. S. *J. Electroceram.* **2009**, *22*, 309–314.
(44) Jitianu, A.; Amatucci, G.; Klein, L. C. *J. Mater. Res.* **2008**, *23*, 2084–2090.
(45) Monde, T.; Fukube, H.; Nemoto, F.; Yoko, T.; Konakahara, T. *J. Non-Cryst. Solids* **1999**, *246*, 54–64.
(46) Bhagat, S. D.; Oh, C.-S.; Kim, Y. H.; Ahn, Y.-S.; Yeo, J.-G. *Microporous Mesoporous Mater.* **2007**, *100*, 350–355.
(47) Rao, A. V.; Kulkarni, M. M.; Amalnerkar, D. P.; Seth, T. *J. Non-Cryst. Solids* **2003**, *330*, 187–195.
(48) Quere, D. *Physica A* **2002**, *313*, 32–46.
(49) Chau, T. T.; Bruckard, W. J.; Koh, P. T. L.; Nguyen, A. V. *Adv. Colloid Interface Sci.* **2009**, *150*, 106–115.

As shown in previous studies from our group[33,50] and from the Brennan group,[51] microscopically heterogeneous films are often obtained from mixtures of separately hydrolyzed sols. Future studies of these gradients will include investigations of such heterogeneity by implementation of atomic force and single molecule microscopy methods.

(50) Striova, J.; Higgins, D. A.; Collinson, M. M. *Langmuir* **2005**, *21*, 6137–6141.
(51) Goring, G. L. G.; Brennan, J. D. *Chem. Mater.* **2007**, *19*, 5336–5346.

Acknowledgment. The authors gratefully acknowledge the support of the National Science Foundation (CHE-0647849 and CHE-0648716) in these studies. Jim Hodgson, Bruce Law, and Takashi Ito are thanked, respectively, for help with the "infusion-withdrawal dip-coating" apparatus, water contact angle measurements, and use of the spectroscopic ellipsometer.

Supporting Information Available: Surface roughness data for a 1:10 MTMOS gradient and NR fluorescence spectra in one- and two-component nongradient films (PDF). This material is available free of charge via the Internet at http://pubs.acs.org.